




Crossover from proximity to ordinary two-dimensional plasma excitation

V. M. Muravev, I. V. Andreev , N. D. Semenov , S. I. Gubarev, and I. V. Kukushkin
Institute of Solid State Physics, RAS, Chernogolovka 142432, Russia

 (Received 27 January 2021; revised 11 March 2021; accepted 12 March 2021; published 26 March 2021)

We have investigated plasma excitations in a disk-shaped two-dimensional electron system (2DES), the edge of which was covered by an overlaying metallic gate. We have found that the microwave response of the structure is dominated by the proximity plasma mode propagating along the disk edge. Significantly, we find that as the overlap between the 2DES and the gate tends to zero, the frequency of the proximity plasmon makes a transition to that of an ordinary 2D plasmon in the ungated area of the 2DES. We also observe that tuning the electron density under the gate results in a crossover from the proximity to the laterally screened 2D plasmon. The experimental findings are analyzed using the plasmonic lumped-element approach.

DOI: [10.1103/PhysRevB.103.125308](https://doi.org/10.1103/PhysRevB.103.125308)

I. INTRODUCTION

Plasma excitations in two-dimensional electron systems (2DESs) have been the subject of active research in recent years [1–7]. The surge of interest in 2D plasmonics has been encouraged by a number of latest promising results. One of them is the discovery of a new family of two-dimensional plasma excitations—proximity plasmons [8–13]—observed when a metal strip is placed in proximity to a 2DES. For these particular waves, the plasmon wave vector is directed along the gate strip, with no potential nodes present in the transverse direction. Furthermore, it was found [8] that the spectrum of the proximity plasmon combines the unique features of gated plasmons with $\omega_g \propto \sqrt{h}$ [14], where h is the distance between the gate and the 2DES, and ungated plasma excitations with $\omega_p \propto \sqrt{q}$ [15], as follows,

$$\omega_{\text{pr}}(q) = \sqrt{\frac{2n_s e^2 h}{m^* \epsilon \epsilon_0} \frac{q}{W}} \quad (qW \ll 1), \quad (1)$$

where n_s is the 2D electron density, m^* is the effective electron mass, $q = 2\pi/\lambda$ is the plasmon wave vector directed along the infinite gate, W is the gate strip width, ϵ_0 is the electric constant, and ϵ is the effective dielectric permittivity of the semiconductor crystal between the 2DES and the gate. Formula (1) was obtained under the assumption that $h \ll W$ and $h \ll \lambda$. In the present paper, we consider a semi-infinite 2DES with the gate strip partially overlapping the electron system along the edge. In this case the frequency ω_{pr} from (1) is scaled down by a factor of $\sqrt{2}$ [8,10]. The given geometry is very similar to that of a high-electron-mobility transistor (HEMT). Interestingly, the proximity plasmon frequencies in industrial HEMTs lie in the terahertz range—the region of the electromagnetic spectrum that remains most unexploited by technological developments [9]. Therefore, proximity plasmons in HEMT devices can be used to amplify the incident electromagnetic field, boosting the sensitivity of terahertz detectors [16–21].

Even though the proximity plasmon wave propagates along the gate strip, its wave motion involves mostly electrons from the ungated 2DES area of $\lambda \times \lambda$ [8]. This has two physical consequences. First, in the limit of $\lambda \gg W$, the proximity plasmon frequency is expected to be weakly dependent on the electron density under the gate. Second, the proximity plasma wave should interact with the 2D plasma in the ungated area of the 2DES. Both of these properties have not been studied previously. Thus, in the present paper, we examine the interaction between proximity plasma excitations and an ungated 2D plasma. We trace how the proximity plasma excitation crosses over to the ungated plasmon whenever the gate width is decreased or the 2DES under the gate is depleted. Moreover, by changing the biasing gate voltage, we demonstrate that the proximity plasmon frequency is unaffected by the electron density under the gate. This observation proves that the proximity wave motion is localized in the ungated 2DES region, whereas the electric field energy of the wave is stored in the gate-2DES gap.

II. EXPERIMENTAL TECHNIQUE

The experiments were conducted on a GaAs/AlGaAs heterostructure with a 30-nm-wide quantum well located at a distance of $h = 440$ nm beneath the crystal surface. Between different samples, the electron density n_s was varied in the range of $(2.5\text{--}3.0) \times 10^{11} \text{ cm}^{-2}$. At $T = 1.5$ K, the system had a transport electron mobility $\mu = 5 \times 10^6 \text{ cm}^2/\text{V s}$. The given heterostructure was used to fabricate several disk-shaped mesas with diameters of 900, 700, 600, 520, and 510 μm . The metallic gate—a 1×1 mm Au/Cr square with a concentric circular aperture of diameter $D = 0.5$ mm—was thermally deposited on top of the mesa, as illustrated in Fig. 1. For different samples, the amount of overlap between the gate and the mesa was set to $W = 200, 100, 50, 10,$ and $5 \mu\text{m}$. For comparison, two types of structures were fabricated: one with an Au/Ge ohmic contact added at the gate cutout [Fig. 1(a)] to enable control of the 2DES electric potential, and the other

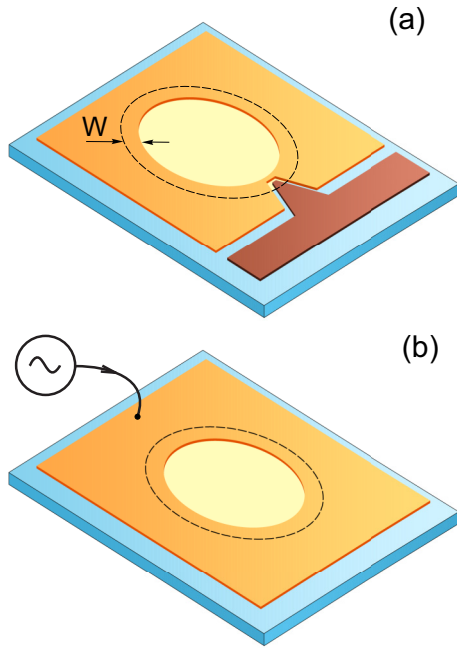


FIG. 1. Schematic drawing of two types of experimental structures. (a) A disk-shaped mesa (yellow) partially covered by an overlaying metallic gate (orange). A contact electrode (brown) cut in the gate is used to control the 2DES potential. (b) Configuration with the mesa and the gate only. The dashed line marks the boundary of the 2DES underneath the gate.

with no contact electrode [Fig. 1(b)]. Plasma waves were excited by microwave radiation being fed directly to the gate through a coaxial cable. A DC bias voltage could be applied directly between the gate and the grounded ohmic contact to deplete the 2DES beneath the gate. In our experiments, the gate was kept DC grounded (only a microwave AC potential was applied to the gate), and a positive DC bias was applied to the 2DES via an ohmic contact. Therefore, the potential of the gate relative to 2DES was negative or zero. Since the gate potential relative to 2DES was controlled directly, we assume the charge distribution under the gate is uniform. To detect the microwave absorption in the 2DES, we employed an advanced noninvasive optical technique [22]. All measurements were conducted at a temperature $T = 1.5$ K, with a magnetic field $B = 0$ –2 T applied perpendicular to the sample surface. The samples were immersed in a liquid helium cryostat at the center of the superconducting coil.

III. RESULTS AND DISCUSSION

A. Proximity plasmon dispersion

Figure 2(a) shows microwave absorption measured as a function of the magnetic field. The lower two curves denote the measurements at $f = 4.2$ and 6.0 GHz carried out on the sample structure in Fig. 1(a), with an electron density $n_s = 3.0 \times 10^{11} \text{ cm}^{-2}$, and an overlap width $W = 50 \mu\text{m}$. These data reveal a set of resonances symmetric with respect to the sign of the magnetic field. The resulting magnetic-field behavior of the resonances is displayed in Fig. 2(b). The obtained magnetodispersion reveals that observed resonances

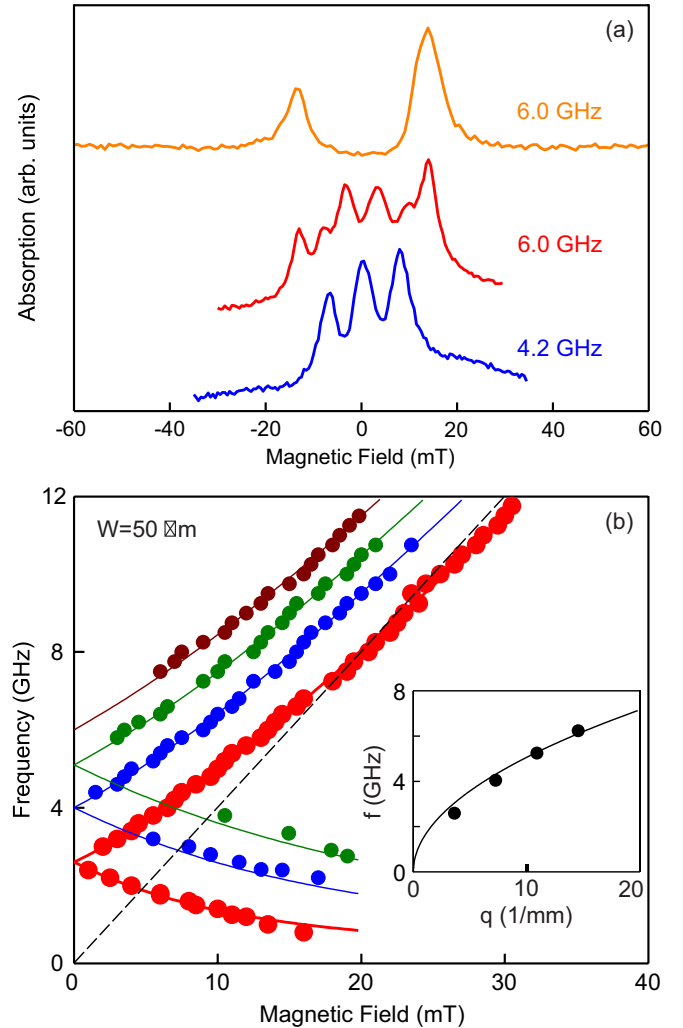


FIG. 2. (a) Microwave absorption as a function of the B field, measured at 4.2 and 6 GHz for the sample with an ohmic contact in Fig. 1(a), and at 6 GHz (the upper curve) for the sample with a uniform gate in Fig. 1(b). Both samples have the same geometrical dimensions $W = 50 \mu\text{m}$ and $D = 0.5 \text{ mm}$, as well as 2D electron density $n_s = 3.0 \times 10^{11} \text{ cm}^{-2}$. The plots are offset for clarity. (b) Magnetodispersion of the first four proximity plasmon modes excited in the sample by the contact finger. Solid lines represent fitted curves according to Eq. (2). The dashed line corresponds to the cyclotron resonance $\omega_c = eB/m^*$. The inset shows the proximity plasmon spectrum at $B = 0$ T, with the solid line denoting the theoretical prediction according to Eq. (1).

correspond to excitation of a family of plasmon modes with a fundamental plasma frequency of $f_p = 2.5$ GHz. Hence, we can assign each mode a wave vector $q_N = 2N/(D + W)$, where $N = 1, 2, 3, 4$ is the mode number. This wave-vector quantization condition comes from the fact that the mean perimeter of the gated ring $\pi(D + W)$ has to be equal to an integer number of plasmon wavelengths. Then, we can reconstruct the dispersion of the plasma wave under study, as indicated in the inset in Fig. 2(b). Importantly, the measured dispersion closely follows the spectrum of the proximity plasma predicted by Eq. (1), with $\epsilon = \epsilon_{\text{GaAs}} = 12.8$, as illustrated by the solid curve. It should be noted that there is a

minor discrepancy between the measurement results and the theory, which was also observed in all prior experiments on proximity plasmons [9,10,12]. In the following discussion, we demonstrate that this deviation grows larger with decreasing overlap between the gate and the 2DES—the phenomenon attributed to the interaction of the proximity plasmon with the ungated 2D plasma.

A critical advantage of the structure geometry in Fig. 1(a) is an inhomogeneous electromagnetic field arising in the gap between the contact finger and the gate, which, in fact, enables the excitation of proximity plasmon modes with large wave vectors. To illustrate this, we conducted an independent experiment on the other type of structure with a continuous gate without a cut [Fig. 1(b)]. In this case, the resultant microwave absorption indicates only the lowest $N = 1$ proximity plasma mode, as shown by the upper curve in Fig. 2(a).

We also note that in Fig. 2(b), each mode has two branches—one with positive and one with negative magnetodispersion. The same magnetic-field behavior is observed for the fundamental plasmon mode excited in a disk geometry [23]. With application of a magnetic field the plasma resonance splits into two. As the magnetic field is raised, one mode ω_+ approaches the cyclotron resonance, and the low-frequency edge mode ω_- tends toward zero frequency [23,24],

$$\omega_{\pm} = \pm \frac{\omega_c}{2} + \sqrt{\frac{\omega_c^2}{4} + \omega_p^2}, \quad (2)$$

where $\omega_c = eB/m^*$ is the cyclotron frequency. It should be mentioned that according to our measurements, the upper magnetoplasmon mode intersects the cyclotron resonance line. This behavior can be explained by the retardation effects that reduce the value of the effective cyclotron frequency used in Eq. (2) to fit the experimental data [25].

B. Gate tuning experiments

Figure 3 summarizes the magnetic-field behavior of the $N = 1$ proximity plasmon frequency in a frequency range up to 40 GHz. Importantly, we determine how the 2DES density under the gate influences the proximity plasmon frequency by applying a positive bias voltage to the 2DES using the ohmic contact while keeping the gate DC grounded. Thus, the voltage at the gate U_g relative to 2DES was negative. For the reference measurement at zero gate voltage $U_g = 0$ V, the 2DES density was $n_s = 3.0 \times 10^{11} \text{ cm}^{-2}$. Then, it was estimated that changing the gate voltage by $\Delta U_g = 1$ V leads to $\Delta n_s = (\epsilon_0 \epsilon / eh) \Delta U_g = 1.7 \times 10^{11} \text{ cm}^{-2}$. As a result, the data curves in Fig. 4 indicate that the $N = 1$ proximity plasma mode remains practically unchanged when the 2DES density under the gate is depleted tenfold, from the initial level at $U_g = 0$ V (blue curve) to $n_s = 0.3 \times 10^{11} \text{ cm}^{-2}$ at $U_g = -1.6$ V (green curve). Detailed magnetodispersions for $n_s = 0.3 \times 10^{11} \text{ cm}^{-2}$ and $1.3 \times 10^{11} \text{ cm}^{-2}$ are provided in the Supplemental Material [26].

According to Fig. 4, a further depletion, corresponding to $U_g = -2.1$ and -2.5 V, causes an abrupt shift in the resonance position, as illustrated by the black and red curves,

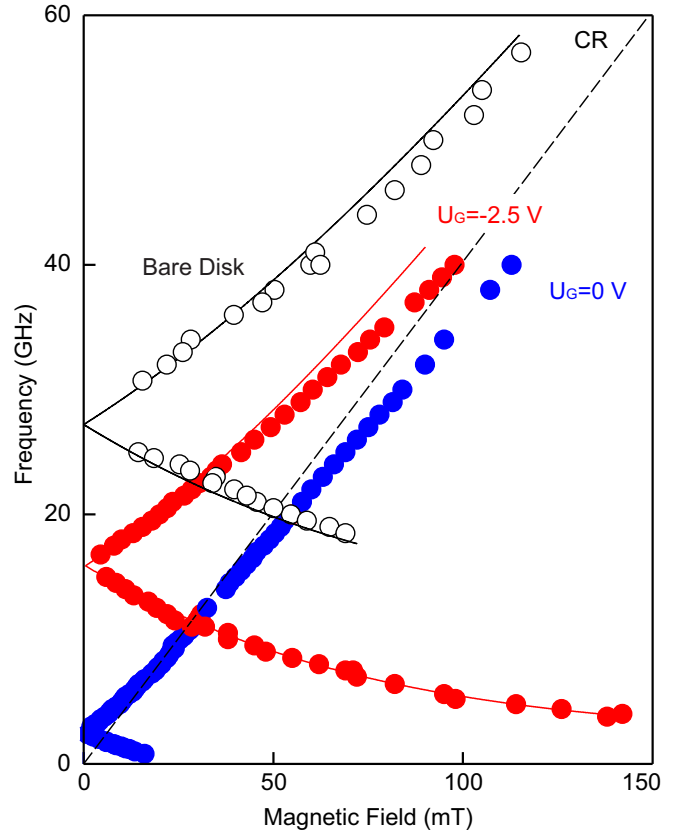


FIG. 3. Dependence of the magnetoplasma resonance frequency on the applied magnetic field. Measurement data for a bare, ungated 2DES disk of diameter $d = 0.5$ mm (open circle); the gated structure in Fig. 1(a) with gate aperture diameter $D = 0.5$ mm, and overlap width $W = 50 \mu\text{m}$. Voltage $U_g = -2.5$ V completely depletes electrons under the gate (solid red circle); the same structure at $U_g = 0$ V, with the same 2DES density $n_s = 3.0 \times 10^{11} \text{ cm}^{-2}$ both in the aperture region and under the gate (solid blue circle). The respective solid curves are calculated from Eq. (2). The dashed line is the magnetic-field dependence of the cyclotron frequency $\omega_c = eB/m^*$.

respectively. This event corresponds to the total depletion of two-dimensional electrons in the region under the gate. As a result, we arrive at the 2DES disk of diameter D , which is laterally screened by the gate. In this configuration, only the fundamental plasma mode can be excited, with a charge fluctuation across the disk. Notably, we observe only a single plasma mode at any gate voltage. The dispersion relation of this plasma excitation is modified in a wide range by the boundary condition imposed by the gate. Indeed, the plasmon magnetodispersion at complete depletion ($U_g = -2.5$ V) exhibits a similar pattern of two branches converging to $f_p = 15.8$ GHz at zero magnetic field, as indicated by the red circles in Fig. 3. For comparison, the open circles in the same figure show the plasmon magnetodispersion measured on a bare disk of diameter $D = 0.5$ mm fabricated on the same wafer. Lateral screening leads to the softening of the plasmon frequency by $\alpha = 1.7$. The estimated screening factor is in good agreement with theoretical calculations [27–31] and previous experiments [32].

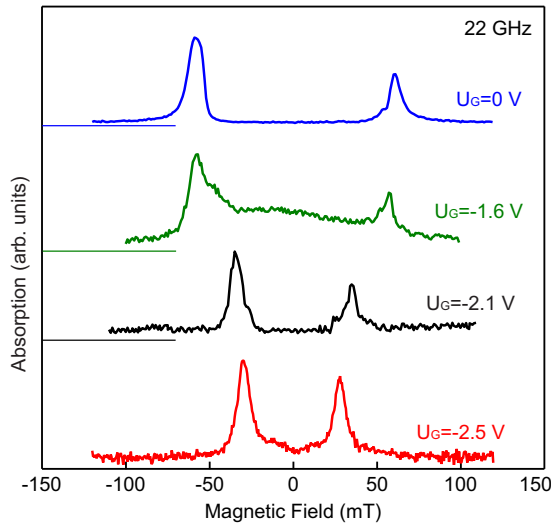


FIG. 4. Microwave absorption at 22 GHz as a function of the magnetic field, measured at the gate voltages $U_g = 0, -1.6, -2.1,$ and -2.5 V, for a fixed gate-2DES overlap width $W = 50 \mu\text{m}$ and electron density $n_s = 3.0 \times 10^{11} \text{cm}^{-2}$. The curves are offset vertically for clarity.

C. Experiments on the structures with different gate-2DES overlap

The described gate-tuning experiment allowed us to observe the crossover from the proximity to an ordinary laterally screened 2D plasma excitation. However, the demonstrated transition is fairly abrupt. Another way to trace the crossover is to vary the overlap width W . To do that, we fabricated five samples with a fixed aperture diameter $D = 0.5$ mm and $n_s = 3.0 \times 10^{11} \text{cm}^{-2}$, but different widths of the gate-2DES overlap $W = 200, 100, 50, 10,$ and $5 \mu\text{m}$. In Fig. 5, we plot the $N = 1$ proximity plasmon frequency as a function of

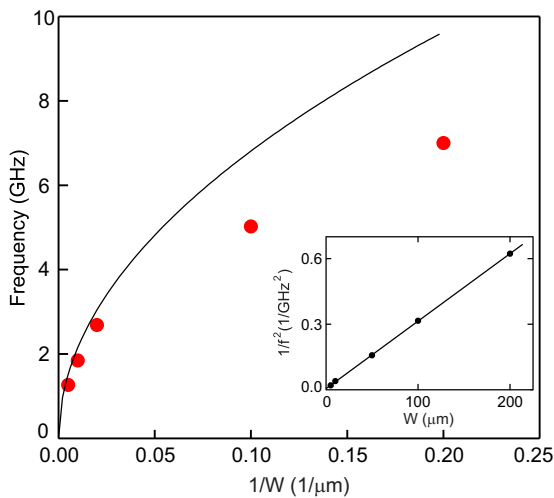


FIG. 5. Proximity plasmon frequency as a function of the inverse overlap width $1/W$. Measurements are taken from five samples fabricated from the same wafer with $n_s = 3.0 \times 10^{11} \text{cm}^{-2}$. The solid line indicates the theoretical prediction according to Eq. (1). The inset shows the plot of the same data as $1/f^2$ vs W .

$1/W$, where each data point corresponds to the measurement from a single sample. For large overlap values, $W = 200$ and $100 \mu\text{m}$, experimental data closely follow the dispersion of the proximity plasmon (1) denoted by the solid line. However, in the small- W limit, the measurement results significantly deviate from the theoretical curve, consistent with a similar discrepancy reported in previous experimental studies [9,10,12,13]. It indicates that the proximity plasmon enters a new regime when its dynamics is dominated by the ungated 2D plasma. Again, we observe only a single plasma resonance, which suggests a continuous transition from the proximity to an ordinary 2D plasmon. The proximity and ungated plasmons do not coexist simultaneously in our experiments.

The easiest way to quantitatively understand this result is to treat the proximity plasma wave in terms of the lumped-element approach [33–35]. In this approach, the impedance of the 2D plasma at zero magnetic field can be expressed as follows:

$$Z_{2\text{DES}}(\omega) = R + i\omega L_K, \quad L_K = \frac{m^*}{n_s e^2}. \quad (3)$$

Here, the impedance is derived based on the Drude conductivity model, $Z_{2\text{DES}}(\omega) = 1/\sigma(\omega) = (1 + i\omega\tau)m^*/n_s e^2\tau$, where τ is the transport relaxation time, and L_K is the kinetic inductance of nonmagnetic origin, due to the inertia of the electrons. Considering that the gated region of the 2DES acts as an equivalent capacitor,

$$C = \frac{\varepsilon\varepsilon_0 W}{hq}, \quad (4)$$

the resonant frequency of the equivalent LC plasmonic circuit becomes

$$\omega_{\text{pr}} = \frac{1}{\sqrt{L_K C}} = \sqrt{\frac{n_s e^2 h q}{m^* \varepsilon\varepsilon_0 W}}, \quad (5)$$

which reproduces dispersion of the proximity plasmon given by Eq. (1).

The next step is to account for the extra “lateral” capacitance C_{lat} due to the screening charges accumulated in the ungated area of the 2DES. The total capacitance is the sum of two terms $C + C_{\text{lat}}$, leading to the following plasma frequency:

$$\omega_p = \frac{1}{\sqrt{L(C + C_{\text{lat}})}}. \quad (6)$$

Going back to Fig. 5, we see that for the large values of the gate-2DES overlap ($1/W \rightarrow 0$), the total capacitance is dominated by $C \gg C_{\text{lat}}$. In this limit, the experimental points follow closely the theoretical dependence (5). On the other hand, in the opposite case of $1/W \rightarrow \infty$, the lateral capacitance $C_{\text{lat}} \gg C$, and the proximity mode is transformed into an ordinary 2D plasma mode with frequency $\omega_0 = 1/\sqrt{L C_{\text{lat}}}$. To determine ω_0 , we plot the same data as $1/f^2$ vs W , as shown in the inset in Fig. 5. The experimental data closely follow the linear dependency, with the extrapolation to $W = 0$ yielding $f_0 = (14 \pm 3)$ GHz (see Supplemental Material for details [26]). The found frequency is very close to 15.8 GHz—the frequency of a laterally screened plasmon in a disk of

diameter $D = 0.5$ mm. Therefore, by gradually decreasing W , we achieved a continuous crossover from the proximity to an ordinary ungated 2D plasma excitation.

IV. SUMMARY AND CONCLUSION

In conclusion, we have experimentally studied the properties of collective excitations in a 2D electron disk, partially covered on the perimeter by an overlaying gate. In particular, we have investigated the transformation of the proximity 2D magnetoplasmon into that of an ordinary one by two different approaches. First, we took measurements from a set of samples with the same aperture diameter and electron density but varied width of the gate-2DES overlap. Then, we used the other approach of continuously tuning the 2D density under the gate. We have shown that partial depletion of electron

density in the region under the gate has a negligible effect on the proximity plasmon frequency. In turn, total depletion results in significant changes in the dispersion, which signal a crossover from a proximity to a laterally screened 2D plasmon. We demonstrate that decreasing the width of the gate-2DES overlap leads to the same crossover effect. Our experimental findings are confirmed qualitatively using a plasmonic lumped-element model.

ACKNOWLEDGMENTS

We thank V. A. Volkov and A. A. Zabolotnykh for the stimulating discussions. The authors gratefully acknowledge the financial support from the Russian Science Foundation (Grant No. 18-72-10072).

-
- [1] W. F. Andress, H. Yoon, K. Y. M. Yeung, L. Qin, K. West, L. Pfeiffer, and D. Ham, *Nano Lett.* **12**, 2272 (2012).
- [2] J. Chen, M. Badioli, P. Alonso-Gonzalez, S. Thongrattanasiri, F. Huth, J. Osmond, M. Spasenovic, A. Centeno, A. Pesquera, P. Godignon, A. Zurutuza Elorza, N. Camara, F. Abajo, R. Hillenbrand, and F. H. L. Koppens, *Nature (London)* **487**, 77 (2012).
- [3] Z. Fei, A. S. Rodin, G. O. Andreev, W. Bao, A. S. McLeod, M. Wagner, L. M. Zhang, Z. Zhao, M. Thiemens, G. Dominguez, M. M. Fogler, A. H. Castro Neto, C. N. Lau, F. Keilmann, and D. N. Basov, *Nature (London)* **487**, 82 (2012).
- [4] G. C. Dyer, G. R. Aizin, S. J. Allen, A. D. Grine, D. Bethke, J. L. Reno, and E. A. Shaner, *Nat. Photonics* **7**, 925 (2013).
- [5] J. Lusakowski, *Semicond. Sci. Technol.* **32**, 013004 (2016).
- [6] Q. Shi, M. A. Zudov, L. N. Pfeiffer, K. W. West, J. D. Watson, and M. J. Manfra, *Phys. Rev. B* **93**, 165438 (2016).
- [7] D. A. Bandurin, D. Svinsov, I. Gayduchenko, S. G. Xu, A. Principi, M. Moskotin, I. Tretyakov, D. Yagodkin, S. Zhukov, T. Taniguchi, K. Watanabe, I. V. Grigorieva, M. Polini, G. N. Goltsman, A. K. Geim, and G. Fedorov, *Nat. Commun.* **9**, 5392 (2018).
- [8] A. A. Zabolotnykh and V. A. Volkov, *Phys. Rev. B* **99**, 165304 (2019).
- [9] V. M. Muravev, P. A. Gusikhin, A. M. Zarezin, I. V. Andreev, S. I. Gubarev, and I. V. Kukushkin, *Phys. Rev. B* **99**, 241406(R) (2019).
- [10] V. M. Muravev, A. M. Zarezin, P. A. Gusikhin, A. V. Shupletsov, and I. V. Kukushkin, *Phys. Rev. B* **100**, 205405 (2019).
- [11] A. A. Zabolotnykh and V. A. Volkov, *Semiconductors* **53**, 1870 (2019).
- [12] A. M. Zarezin, P. A. Gusikhin, V. M. Muravev, and I. V. Kukushkin, *Pis'ma Zh. Eksp. Teor. Fiz.* **111**, 316 (2020) [*JETP Lett.* **111**, 282 (2020)].
- [13] V. M. Muravev, P. A. Gusikhin, A. M. Zarezin, A. A. Zabolotnykh, V. A. Volkov, and I. V. Kukushkin, *Phys. Rev. B* **102**, 081301(R) (2020).
- [14] A. V. Chaplik, *Zh. Eksp. Teor. Fiz.* **62**, 746 (1972) [*Sov. Phys. JETP* **35**, 395 (1972)].
- [15] F. Stern, *Phys. Rev. Lett.* **18**, 546 (1967).
- [16] M. Dyakonov and M. Shur, *Phys. Rev. Lett.* **71**, 2465 (1993).
- [17] W. Knap, Y. Deng, S. Romyantsev, J.-Q. Lú, M. S. Shur, C. A. Saylor, and L. C. Brunel, *Appl. Phys. Lett.* **80**, 3433 (2002).
- [18] E. A. Shaner, M. Lee, M. C. Wanke, A. D. Grine, J. L. Reno, and S. J. Allen, *Appl. Phys. Lett.* **87**, 193507 (2005).
- [19] G. R. Aizin, V. V. Popov, and O. V. Polishchuk, *Appl. Phys. Lett.* **89**, 143512 (2006).
- [20] V. M. Muravev and I. V. Kukushkin, *Appl. Phys. Lett.* **100**, 082102 (2012).
- [21] O. Sydoruk, J. B. Wu, A. Mayorov, C. D. Wood, D. K. Mistry, and J. E. Cunningham, *Phys. Rev. B* **92**, 195304 (2015).
- [22] I. V. Kukushkin, J. H. Smet, K. von Klitzing, and W. Wegscheider, *Nature (London)* **415**, 409 (2002).
- [23] S. J. Allen, H. L. Störmer, and J. C. M. Hwang, *Phys. Rev. B* **28**, 4875 (1983).
- [24] A. L. Fetter, *Phys. Rev. B* **32**, 7676 (1985).
- [25] I. V. Kukushkin, J. H. Smet, S. A. Mikhailov, D. V. Kulakovskii, K. von Klitzing, and W. Wegscheider, *Phys. Rev. Lett.* **90**, 156801 (2003).
- [26] See Supplemental Material at <http://link.aps.org/supplemental/10.1103/PhysRevB.103.125308> for the experimental study of the fundamental plasmon mode in the samples at different gate bias voltages and the details of the estimation of lateral capacity from the experimental data.
- [27] V. Ryzhii, A. Satou, I. Khmyrova, A. Chaplik, and M. S. Shur, *J. Appl. Phys.* **96**, 7625 (2004).
- [28] A. Satou, V. Ryzhii, and A. Chaplik, *J. Appl. Phys.* **98**, 034502 (2005).
- [29] S. A. Mikhailov and N. A. Savostianova, *Phys. Rev. B* **74**, 045325 (2006).
- [30] A. Satou and S. A. Mikhailov, *Phys. Rev. B* **75**, 045328 (2007).
- [31] V. V. Popov, O. V. Polishchuk, and S. A. Nikitov, *Pis'ma Zh. Eksp. Teor. Fiz.* **95**, 91 (2012) [*JETP Lett.* **95**, 85 (2012)].
- [32] S. I. Gubarev, A. A. Dremin, V. E. Kozlov, V. M. Murav'ev, and I. V. Kukushkin, *Pis'ma Zh. Eksp. Teor. Fiz.* **90**, 588 (2009) [*JETP Lett.* **90**, 539 (2009)].
- [33] P. J. Burke, I. B. Spielman, J. P. Eisenstein, L. N. Pfeiffer, and K. W. West, *Appl. Phys. Lett.* **76**, 745 (2000).
- [34] G. R. Aizin and G. C. Dyer, *Phys. Rev. B* **86**, 235316 (2012).
- [35] V. M. Muravev, N. D. Semenov, I. V. Andreev, P. A. Gusikhin, and I. V. Kukushkin, *Appl. Phys. Lett.* **117**, 151103 (2020).